A chemically defined system supports two distinct types of stem cell from a single blastocyst and their self-assembly to generate blastoid

Siqin Bao (baosq@imu.edu.cn)
Inner Mongolia University https://orcid.org/0000-0002-9582-3194
Baojiang Wu
Inner Mongolia University
Zhiqing Yang
Inner Mongolia University
Yijie Liu
Inner Mongolia University
Jianwen Li
Inner Mongolia University
Chen Chen
Inner Mongolia University
Xihe Li
Inner Mongolia University

Article

Keywords:

Posted Date: July 19th, 2022

DOI: https://doi.org/10.21203/rs.3.rs-1773687/v1

Abstract

The pluripotent stem cells exist in a narrow window during early development and its derivation depends on intrinsic and extrinsic growth signaling *in vitro*. It has remained challenging to derive two or three distinct cell lines that are representative of blastocyst-stage lineages from one preimplantation embryo simultaneously in a chemical defined condition. Therefore, it is desirable to establish a system by manipulating extrinsic signaling in culture to derive multiple types of stem cells from a single blastocyst. Here, we report that a defined medium containing Activin A, WNT activator and LIF (ACL medium), enables establishment of ACL-ESCs and ACL-XEN cells from one blastocyst. Our results indicate that ACL-ESCs and ACL-XEN cells represent ICM and PrE lineages of blastocyst. Importantly, we obtained ACL-blastoid from ACL-ESCs and ACL-XEN cells self-aggregation, partially recapitulating early development and initiation of early implantation events. This study would not only provide a culture system for derivation and maintenance of two types of cell lines corresponding to ICM as well as PrE, but also deepen our understanding of early embryogenesis and widen insights into translational application of stem cells.

Introduction

During early stage of embryogenesis in mammals, the development potential of cells in the embryo is gradually restricted with a series of cleavage and early differentiation. It is an initial cell fate commitments during morula compaction that outer cells segregate from the blastomeres as trophectoderm (TE) which surround inner cell mass (ICM), hence the blastocyst is formed following cavitation. Prior to implantation, the inner cell mass generates both epiblast progenitor cells and the bipotent extra-embryonic primitive endoderm (PrE) which differentiates into endodermal lineages, the parietal and visceral endoderm (PE and VE) [1-3].

Three representative stem cells derived from blastocysts are able to self-renew, maintain and proliferate *in vitro* as embryonic stem cells (ESCs) [4-6], trophoblast stem cells (TSCs) [7] and extraembryonic endoderm stem cells [8, 9], respectively. ESCs derive and maintain properties as self-renewal and pluripotency by addition of two small molecule inhibitors of glycogen synthase kinase 3 and mitogen-activated protein kinase (2i), and leukemia inhibitory factor (LIF) [6]. Only ESCs have be confirmed through the gold-standard germline transmission test and can give rise to all tissues of the body [10]. TSCs are derived from the trophoblast and maintained *in vitro* in the presence of FGF4 and heparin while retaining the ability to differentiate into multiple cell types of the placenta [7, 11, 12]. XEN cells can be established and continuously passaged using same TSCs culture condition or medium containing serum, contribute to the extraembryonic endoderm cell types [13, 14].

Respectively, all three cell lineages are maintained indefinitely in their particular cell culture system as stable cell lines with essential signal requirements, whereas there are still certain interactions among them. Trophectoderm is specified due to the compaction during morula and restricted in its developmental potential with the expression of genes related to trophectoderm, which is distinguished

from pluripotent inner cell mass as well as ESCs, the corresponding cell lineages of ICM *in vitro*. However, it is reported that ICM [15] and ESCs [16] still have the ability to partially differentiate into trophoblast lineages. Trophectoderm can be induced by the ectopic expression of the caudal-type homeobox transcription factor 2 (Cdx2) from ESCs. And not coincidentally, overexpression of Gata4 or Gata6 in ESCs is sufficient to induce the establishment of self-renewing XEN cells which is the *in-vitro* counterpart of the PrE lineage of the mouse embryo [17, 18]. In fact, it has been found that XEN-like cells exist within mESC cultures and can be induced to proliferate during the XEN protocol [4, 19]. XEN cells of human or mouse are able to be derived from ESCs by addition of endoderm agonists Activin + WNT, and expand in the presence of LIF and low insulin without the requirement for gene manipulation [20, 21], likewise, retinoic acid (RA) and ActA applying progressively to ESCs can also promote differentiation of XEN cells in mice [22]. Moreover, although TS cell colonies were present during the process of XEN cell lines derivation from ICM or single blastocysts within TSCs derivation condition [7, 8], in which FGF4 is required for derivation but not necessary for XEN cell maintenance, XEN cells are still dominant group in comparison. Altogether, it is suggested that all three blastocyst lineages are not separated completely, but communicate with each other by using a handful of conserved signaling pathways. As representative cell lines of blastocyst lineages, ESCs, TSCs and XEN cells were recently applied in combining each other to model the *in vivo* interactions between embryonic and extra-embryonic lineages or being used exclusively in hope of reconstructing embryo-like structures. Early attempts to generate embryo-like structures by spontaneous differentiation of ESCs in suspension culture, this disorganized cell aggregate is termed as embryoid bodies [19, 23]. Reconstruction of embryo-like structures *in vitro* offers new opportunities for understanding embryogenesis. Previous studies have shown that ESCs and TSCs cooperate *in vitro* to form structures resemble embryonic day 3.5 blastocysts, termed blastoids [24]. Furthermore, three kind of stem cells, ESCs, XEN cells and TSCs aggregated together, and formed gastrulating embryo-like structures (or named gastruloids) [25, 26]. Recently, Sozen et al. also demonstrated the generation of blastocyst-like structures from mouse extended pluripotent stem cells (EPSC) aggregated with TSCs that contained three spatially segregated lineages representative of the epiblast, trophectoderm, and primitive endoderm (PrE) [27]. Since three kind stem cells came from different culture medium, it is hard to identify which factors plays an important role for blastoid. The EPSCs could generated blastoid, however the culture medium of EPS-blastoid was complicate, including FGF4, heparin and serum [28]. To understand the precise regulation mechanism of blastoid, it still needs to be further studied.

Several studies also have shown that, human blastocyst-like structures could be generated from human pluripotent stem cells [29, 30] or through iPSC from reprogramming of fibroblasts [28], respectively. Despite embryo-like structures recapitulate key features of early embryonic development, it does not support the development of bona fide embryos. In addition, ESCs have the ability to develop into organoids include gastrulating embryo-like structures that present an invaluable system to recapitulate early development *in vitro* [31-39]. Previous studies indicated that cultures of stem cells could self-assemble *in vitro* to generate gastruloids in human [31]. Although, the most morphological characters and gene expression levels of gastruloids are very similar to the natural embryos, with some difference being the lack of gene expression associated with extra-embryonic cell types [36]. The developmental

defect of stem cell-derived blastoid or gastruloid is mainly associated with the *in vitro* culture conditions, since compared to *in vivo* development, *in vitro* culture conditions is hard to provide the full requirements for stem cell-derived blastoid or gastruloid.

Different signaling pathways provide an important role in development and also control the differentiation into particular germ layers *in vitro*, like Nodal/Activin [40-46], WNT [47-54] , BMP [55-57] and LIF-STAT [58, 59] signaling pathways, especially, which are not only critical for cell lineages derivation and maintenance, but also for generation of embryo-like structures *in vitro*. The precious studies suggested that in mouse, the activation of TGF-β signaling via the ActA pathway supports ESCs proliferation [60], but is also essential for PrE promotion while combinating with CHIR-99021, the stimulator of Wnt signaling, and so does in human ESCs differentiation [20, 21]. CHIR is not only a Wnt/β-catenin agonist but also represses GSK-3 to promote naive pluripotency and diminished variability within cohorts of cells [6]. Besides, in pre-implantation development, LIF-STAT pathway plays a critical role in blocking Epi differentiation, supporting PrE expansion, and correspondingly the maintenance of XEN cell *in vitro*, which is verified that XEN cells derive and proliferate in the condition with EMFIs or EMFI-CM providing an adequate source of LIF [8]. FGF/ERK signaling is required for TE differentiation through Fgfr1 and is also important for PrE specification, which indicates FGF/ERK signaling plays a key role of maintaining appropriate proportions of cell types in the blastocyst [61]. Very recently, researches to induce embryo-like structures by modulating a number signaling pathways has been reported. Bone morphogenetic protein (BMP4), Nodal, STAT, MAPK and WNT signaling are critical to blastoid formation and trophoblast epithelial morphogenesis [24]. Despite WNT signaling pathway is dispensable for blastocyst formation [62, 63], the combination of WNT and FGF4 signaling pathway efficiently reconstruct EPSC-blastoids [28]. Moreover, Nodal/Activin signaling is able to support the development of the extra-embryonic compartment in gastruloid and natural embryos in early post-implantation stages [64]. So far, there are no reports about derivation and maintenance of these three types of stem cell lines which can be applied as the origins of embryo-like structures at the same culture condition. With all the necessary requirements available, it could be possible to generate three types of stem cell lines from one blastocyst by using same culture condition.

Due to restricted accessibility to human embryonic specimens donated to research and ethical limitations, mouse blastocysts were used in this study. [65]Focusing on the Activin A, WNT activator (CHIR99021) and the LIF signaling pathway, we test the hypothesis that there is a defined culture condition sufficient to govern two or three stem cells induction and maintenance . By medium test experiments, we found addition of Activin A, CHIR99021 and LIF (ACL medium), supports establishment two types stem cells, these are ESCs (ACL-ESCs) and XEN-like (ACL-XEN) cells from one blastocyst. Transcriptional characteristics and developmental competence indicated that ACL-ESCs and ACL-XEN cells equivalent to the inner cell mass and primitive endoderm lineages of the pre-implantation embryo. Finally, we show that ACL-ESCs and ACL-XEN cells can self-organize into blastocyst-like structures ACL-blasoids.

Results

Activin A replaces MEK inhibitor to derive ESCs from blastocyst

Early embryonic development is affected by different signaling pathways at different stages of development, however, development of all embryonic cell lineages is happened in the same environment of oviducts or uterus. Therefore, under certain conditions, different types stem cell lines may be generated from single blastocyst. In ESCs culture medium 2i/L (MEK inhibitor PD0325901, GSK3 inhibitor CHIR99021 and LIF), MEK inhibitor PD0325901 prevent ESCs differentiation for long time culture [6]. Nodal/Activin signaling is critical to embryonic development, particular for the extra-embryonic development, we added Activin A to replace MEK inhibitor (PD0325901) in 2i/L medium (Activin A, CHIR99021 and LIF), and named ACL medium, to establish new type embryonic stem cells from blastocyst. The Oct4-△PE-GFP (GOF/GFP, mixed background of MF1, 129/sv, and C57BL/6J strains) 129/sv F1 mice blastocysts were directly placed in chemically defined ACL medium on fibronectin-coated cell culture plate (Fig. 1A). The two types of cells were discovered in ACL medium, one was GOF/GFP positive ESC-like cells, and the other was GOF/GFP negative flat cells in three days culture (Fig. 1B, Supplementary Fig. 1A). We picked GOF/GFP positive cells and digested with Accutase in the further passages, and defined GOF/GFP positive cells as ACL-ESCs. ACL-ESCs were morphologically similar to ESCs and maintained self-renew over passage 50 (p50) (Fig. 1B).

We further determined the key features of ACL-ESCs relative to ESCs. ACL-ESCs exhibited high alkaline phosphatase (AP) activity (Supplementary Fig. 1B) and had normal karyotype (Supplementary Fig. 1C). Immunofluorescence (IF) staining showed that ACL-ESCs expressed pluripotency related proteins OCT4, NANOG, SOX2 and E-cadherin (Fig. 1C). To assesses the *in vivo* developmental potency of ACL-ESCs, we injected ACL-ESCs labeled by H2B tdTomato into eight-cell embryos and investigated chimeric development *in vitro*. The results showed that tdTomato positive ACL-ESCs were contributed robustly to inner cell mass (ICM) (73/73, 100%) and a small number of cells in trophectoderm (TE) (46/73, 63%) region at 48 hours post-injection (Fig. 1D, Supplementary Fig. 1D). However, ACL-ESCs at TE position were exhibited negative for trophectoderm marker CDX2 (Fig. 1E, Supplementary Fig. 1D). Next, we investigated their contribution abilities in chimeric embryos at E6.5, and found that ACL-ESCs were successfully developed to epiblast (19/19, 100%) (Fig. 1F, Supplementary Fig. 1E). Notably, we also obtained full-term chimeras (17/26, 65%) from ACL-ESCs and verified their germline transmission abilities (Fig. 1G, H, Supplementary Fig. 1F). To further define the differentiation ability of ACL-ESCs *in vitro*, 2i/L-ESCs and ACL-ESCs were cultured in N2B27 basic medium without any component, respectively. After undergoing three days of *in vitro* differentiation, the RT-qPCR analysis was performed. Comparing with 2i/L-ESCs, the relative expression of all three germ layer markers were significantly increased in ACL-ESCs except *Hand1* (Supplementary Fig. 1G). These results indicate that ACL-ESCs have strong differentiation ability that depends on changes of environment. All together, these data suggest that Activin A replaces

MEK inhibitor to support derivation of ACL-ESCs from blastocyst, and ACL-ESCs present similar pluripotency features of ESCs and has stronger differentiation ability than ESCs *in vitro*.

ACL culture condition supports XEN cells derivation from blastocyst

When the blastocysts placed in ACL medium for 3–5 days, GOF/GFP positive cells were picked, and GOF/GFP negative flat cells were observed (Fig. 2A). We founded that GOF/GFP negative flat cells were propagated rapidly and they were highly refractile as well as epithelial-like, whose features coincided with typical morphology of XEN cells [8, 13, 14], and designated as ACL-XEN cells (Fig. 2B). ACL-XEN cells showed genome stability after more than 35 passages (Fig. 2B, Supplementary Fig. 2A), and highly expressed primitive endoderm cell lineages related genes such as *Gata4*, *Gata6*, *Sox17* (Supplementary Fig. 2B). IF staining result also indicated that high levels of GATA4 and SOX17 protein were observed in ACL-XEN cells (Fig. 2C).

XEN cells have the capacity to self-renew *in vitro* culture and differentiate into PrE derivatives such as visceral, parietal endoderm, as well as contribute to chimeras (*in vivo*) in a lineage-appropriate manner, showing the developmental potential of their origin [8]. To determine the developmental potential of ACL-XEN cells *in vivo*, we injected ACL-XEN cells with H2B tdTomato to eight-cell stage embryos, and cultured for 48 hours (Supplementary Fig. 2C). The result showed ACL-XEN cells displayed a significant contribution to PrE (18/30, 60%) (Fig. 2D, Supplementary Fig. 2C), and also were co-expressed with GATA4 and SOX17 in chimeras (Fig. 2E). Finally, to confirm whether ACL-XEN cells contribute to visceral endoderm (VE) *in vivo*, we introduced ACL-XEN cells with tdTomato into embryonic day 6.5 (E6.5) and cultured in ACL medium for 48 hours. Interestingly, tdTomato positive cells had the ability to migrate to visceral endoderm for 48 hours culture (Fig. 2F). Above results indicate that ACL condition supports the generation of ACL-ESCs and ACL-XEN cells from one blastocyst with features resembling those of ESCs and XEN cells. Notably, such convenient protocols for deriving XEN cells described here can be completed within 2–3 weeks and without using serum-contained and MEF-conditioned medium [13, 14]. Hence, chemically defined ACL conditions may open new avenues for XEN cell research and help us deepen the understanding of *in vitro* microenvironment for multiple cell lineages development.

Global transcriptional features of ACL-ESCs and ACL-XEN cells

To examine whether ACL-ESCs and ACL-XEN cells have distinct molecular features, RNA sequencing was performed on dynamics of ACL-ESCs and ACL-XEN cells and compared with ESCs [60] and E4.5-PrE [66], respectively. Unsupervised hierarchical clustering (UHC) showed ACL-ESCs close to ACL-XEN cells (Fig. 3A), supporting the two types cell lines derived from the same culture condition. The t-SNE analysis showed that ACL-ESCs and ACL-XEN cells are existed intermediate between ESCs and E4.5-PrE (Fig. 3B). In addition, total of 7,140 genes were differentially expressed in ACL-ESCs compared with ACL-XEN cells, among these 4,372 genes were upregulated in ACL-ESCs (Fig. 3C). Notably, above 4,372 genes are also upregulated in ESCs (Fig. 3C) and Gene ontology (GO) analysis indicated that upregulated genes were

associated with the multicellular organism development, system development and cellular developmental process (Fig. 3D). Another 2,768 genes are upregulated in ACL-XEN cells and GO terms were associated with the bounding membrane of organelle, endomembrane system and organelle membrane (Fig. 3D). These transcriptional profiles show that the gene expression patterns of ACL-ESCs and ACL-XEN cells are closed, but still distinct from each other, and be intermediate between ESCs and E4.5-PrE, respectively.

Furthermore, we used the short time-series expression miner (STEM) method [67] to analyze gene expression profiles on ESCs, ACL-ESCs, ACL-XEN cells and E4.5-PrE. Interestingly, 1,285 differentially expressed genes were significantly highly expressed in ACL-ESCs and ESCs compared with ACL-XEN cells and E4.5-PrE (Fig. 3E). GO terms were associated with ESCs pluripotency such as cell fate commitment, pattern specification process and stem cell differentiation (Fig. 3E). Notably, a total of 309 genes were significantly upregulated in ACL-XEN cells and E4.5-PrE compared with ACL-ESCs and ESCs (Fig. 3E). GO terms were associated with features of XEN cells such as extracellular matrix organization, endoderm development and endoderm formation (Fig. 3E). Meanwhile, a total of 1,187 genes were highly expressed in both ACL-ESCs and ACL-XEN cells (Fig. 3E), these may the ACL condition related target gene, which genes were associated with epigenetic regulation of gene expression, cellular component assembly and vascular smooth muscle contraction processes (Fig. 3E). However, the functional rule of ACL target genes for ACL-ESCs and ACL-XEN cell self-renewal have remains to be further determination. Moreover, as shown in the Venn diagram, ACL-ESCs were more closed to ESCs and ACL-XEN cells are more closed to E4.5-PrE (Fig. 3E). Taken together, these data strongly suggested that the ACL condition can establish and maintain two types of stem cell lines derived from one blastocyst.

Blastocyst-like structures reconstructed from ACL-ESCs and ACL-XEN cells

After fertilization, cleavage stage embryonic cells are able to communicate with each other and developed to blastocyst containing three different cell types (ICM, PrE, and TE) [2]. We next asked whether the two types stem cells derived from one blastocyst (ACL-ESCs and ACL-XEN cells) were cultured together under ACL condition, and be able to aggregate into blastocyst-like structures (or named blastoids) (Fig. 4A). To confirm this hypothesis, we used ACL-ESCs and ACL-XEN cell lines with reporters (GOF/GFP and H2B tdTomato, respectively) to trace their spatial location in further aggregation. When ACL-ESCs and ACL-XEN cells were co-cultured on FN-coated plate with ACL medium, some small clones that epithelial-like cells developed from ACL-XEN cells were surrounding the GOF/GFP positive ACL-ESCs (Supplementary Fig. 3A). We examined the expression of key proteins OCT4 for ACL-ESCs and SOX17 for ACL-XEN cells respectively, and found OCT4 and SOX17 were detectable in co-cultured cells (Supplementary Fig. 3B). Interestingly, some cells co-express OCT4 and SOX17 proteins (Supplementary Fig. 3B), this indicated co-cultured system could drive ACL-ESCs further developed to epiblast and XEN cells. This consistent with the ICM gives rise to the epiblast and extra-embryonic primitive endoderm [2].

Next, we found under these adherent culture condition, co-cultured cells hard to form blastoids structures. Thus, we try to use suspension culture condition, treated cell culture plate by anti-adherence solution [28],

and aggregate two types of stem cell by different cell proportion due to recent reports showed a result of the suitable cell-type proportion and cell-cell communication play an important role in cell proliferation and development [68]. Initially, we aggregated ACL-ESCs and ACL-XEN cells in the proportion of 1:1, 1:5 and 1:10, respectively, and found only mixing ACL-ESCs with ACL-XEN cells at a 1:5 ratio successful induced cavity formation in a small number of cell aggregates, whereas most aggregations failed to form blastoids with a ratio of 1:1, and 1:10 ratio (Fig. 4B, Supplementary Fig. 3C). Using above optimized condition, we consistently observed the development of ACL-blastoids (Fig. 4C), and found its continued to enlarge and reaching an early blastocyst-like size at around day 4. Notably, the average diameter, the total cell number of ACL-blastoids were comparable to E3.5 blastocysts, and the ICM number of ACL-blastoids were higher than E3.5 blastocysts (Fig. 4D, E). In addition, we also tested whether ACL-ESCs and ACL-XEN cell derive blastoids or gastruloids in ETX medium [25]. We found most of cells in ETX medium were differentiated or apoptotic, only a few of cells were able to induce smaller aggregations but failed to form cavity of blastoids or gastruloids morphology (Supplementary Fig. 3D). Collectively, our results demonstrate that ACL-blastoids were reconstructed from ACL-ESCs and ACL-XEN cell aggregation in ACL medium.

ACL-blastoids resemble blastocysts in cell lineage allocation

To investigate whether ACL-blastoid develop to three blastocyst lineages ICM, TE, and PrE as natural E3.5 mouse blastocysts, we performed immunofluorescence. The ACL-blastoids collected on day 5, morphology similar to E3.5 blastocysts. The result revealed that cells on the inside of ACL-blastoid expressed the pluripotency factors OCT4 and SOX2, and the cells on the outer layer of ACL-blastoid expressed the trophectoderm marker CDX2 (Fig. 5A). In addition, we also detected SOX17 positive PrE-like cells surrounding the OCT4 positive compartment, although observed SOX17 positive cells, some of them were mislocated in ACL-blastoids (Fig. 5A). About 81.1% of ACL-blastoids were exhibit SOX2 and CDX2 positive; whereas about 13.2% and 5.7% of ACL-blastoids were only CDX2 or SOX2 positive, respectively (Fig. 5B). These results comparable to previous reported EPS-blastoids [28]. Meanwhile, about 77.4% of ACL-blastoids were exhibit SOX17 and OCT4 positive; whereas about 22.6% of ACL-blastoids were only SOX17 positive (Fig. 5C). We also counted the number of ICM, TE and PrE-like cells in ACL-blastoids (collected at day 5), based on OCT4, SOX2, SOX17 and CDX2 immunostaining. We found that the cell number of OCT4, SOX2 and SOX17 positive cells increased, and CDX2 positive cells decreased in blastoids than E3.5 blastocysts (Fig. 5D, E, Supplementary Fig. 4A). Next, we investigated whether ACL-ESCs and ACL-XEN cells are important for generating blastoids and use 2i/L-ESCs to replace ACL-ESCs and aggregate with ACL-XEN cells in ACL suspension condition. We observed blastocyst-like structures with some GOF/GFP positive cells on the inside, and surrounding by SOX17 positive cells, however without CDX2 positive cells (Supplementary Fig. 4B, C). Furthermore, we also test the possibility of blastoids formation by changing ACL-XEN cells to traditional XEN cells (labeled with tdTomato), and aggregate with ACL-ESCs and 2i/L-ESCs, respectively. But we have not obtained blastocyst-like structures from above two combinations (Supplementary Fig. 4D). These results indicated ACL-ESCs and ACL-XEN cells both are necessary for generation of ACL-blastoids.

Next, as potential autocrine stimuli of self-renewal or differentiation, we examine the requirement for individual pathway stimulation of Activin/Nodal, WNT (CHIR) and STAT3/LIF in ACL-blastoids reconstruction. Addition of inhibitor of Activin/Nodal and STAT3/LIF signaling by SB431542 and JAK inhibitor respectively, they did not affect ACL-blastoids formation (Supplementary Fig. 4E). However, inhibitior XAV939 of WNT signaling caused complete disruption of ACL-blastoids formation (Supplementary Fig. 4E). We conclude canonical WNT signaling was important, but Activin/Nodal and STAT3/LIF signaling was dispensible for ACL-blastoids generating.

Finally, to determine whether key cellular and molecular events feature of early preimplantation development could be recapitulated during ACL-blastoids formation. We traced the dynamics of two types of cell aggregation during the first three days. At day 1 and 2, cells started to form compact aggregates, and the cell adhesion protein E-cadherin began to accumulate at the cell-cell junctions, similar to compacted embryos (Fig. 5F). Importantly, at day 3, started to form blastocyst cavity-like structures (Fig. 5F). In mouse early embryogenesis, TE and ICM lineages are specified from early blastocyst stage and YAP signaling is critical for this process [9, 69–72]. At day 2, YAP could be found in some outside cells of ACL-ESCs and ACL-XEN cell aggregates; at day 3, the nucleus of most outside cells were expressed active YAP protein (Fig. 5G). In addition, we also checked the molecular characteristic of ACL-blastoids (day 4) by qPCR using single ACL-blastoid compared with single blastocyst. We found that some markers of blastocyst lineage expression level were close to natural blastocyst, such as *Rex1*, *Sox17* and *Eomes* (Fig. 5H); but some of three lineage markers *Oct4*, *Nanog*, *Gata6*, *Cdx2*, *Gata2*, *Gata3* were lower in the ACL-blastoids than natural blastocyst (Supplementary Fig. 4F). Together, these findings indicate that ACL-blastoid resembling blastocyst with inner cells expressing pluripotency and outer cells expressing trophectoderm lineage markers.

In Vitro and *in vivo* developmental potential of ACL-blastoids

During embryonic development, early blastomeres are specialized into the ICM and TE, and the ICM gives rise to PrE and epiblast of the blastocysts. Moreover, ESCs, TSCs, and XEN cells can be derived directly from blastocysts [2, 73]. We asked whether ACL-blastoids could also give rise to these three stem cell lines. Here, we successfully generated ESC lines from ACL-blastoids by using 2i/L culture condition. The morphologies of ACL-blastoids derived ESCs are similar to that of natural blastocysts derived ESCs and expressed the pluripotency protein SOX2 (Supplementary Fig. 4G). We also derived TSC lines from ACL-blastoids by using FGF4 and heparin containing conditioned medium on feeder cells and expressed the TS cell key factor CDX2 (Supplementary Fig. 4G). In addition, XEN cell lines were also successfully established from ACL-blastoids and expressed the PrE transcription factors GATA4 (Supplementary Fig. 4G).

Next, we assessed the *in vivo* developmental potential by transferring ACL-blastoids into pseudopregnant mice at 2.5 dpc and 3.5 dpc (Fig. 6A). At 6.5–7.5 dpc, we collected developmental ACL-blastoids, and

found decidua formed in the uteri of surrogates ACL-blastoids (Fig. 6A). Overall, about 17% of transferred ACL-blastoids implanted and induced decidualization (Fig. 6A, B). However, only about 2% of transferred ACL-blastoids form gastrulation-like structure (Fig. 6C). Although ACL-blastoids can successfully form gastrulation-like structure, the size of gastrulation-like structure was varied and much smaller than that of control (Fig. 6B). Importantly, IF results indicated that deciduae induced by gastrulation-like structures were presence of SOX2, GATA6, and CDX2 positive cells (Fig. 6D). Meanwhile, lumenogenesis in the post-implantation embryos are regulated by podocalyxin (PCX) [74]. PCX, cell adhesion protein E-cadherin, and N-cadherin levels were also detected in deciduae derived from ACL-blastoids (Fig. 6E), whereas the distribution pattern of PCX, E-cadherin, and N-cadherin were disorganized in deciduae derived from ACL-blastoids. Furthermore, whether artificial embryos have the developmental ability resemble natural embryos remains to be further studied. In summary, ACL-blastoids could give rise to ESCs, TSCs, and XENs *in vitro* and, could develop into gastrulation-like structure *in vivo* (Fig. 6F).

Discussion

Mice pluripotent stem cells have been established in different medium with overlapping components. Ying et al. noted that inhibition of Mek1/2 (PD) and Gsk3b (CHIR), as well as activation of STAT3/LIF signaling, known as 2i/L medium enhance the derivation of ESCs and promote ground-state pluripotency [6]. Whereas it is permissive for XEN cells promoting from ESCs when CHIR cooperates with Activin A. As it reported, the establishment of epiblast-derived stem cells (EpiSCs), a pluripotent cell type, needs the existence of fibroblast growth factor (FGF) and Activin A [77, 78]. The maintaining of TSCs and XEN cells depend on the Activin/Nodal and FGF signaling [7, 8]. Previous study also indicated that prolonged Mek1/2 suppression impairs the chromosomal stability of ESCs [79], the cytokine LIF, which potently promotes mouse ESC identity, is a key component of ESCs culture conditions [80, 81], while the LIF-STAT pathway may be also playing a role in XEN cell maintenance with the expression of some components as LIFR, gp130, JAK1, JAK2, STAT1 and STAT3 [8]. Our study also shows that LIF alone is sufficient to maintain ESCs pluripotency with hypermethylated state [82]. Considered above research, we indicated Activin/Nodal, CHIR and LIF (ACL medium) are sufficient to derived two type distinct stem cell lines from blastocysts. However, how cell linages of blastocysts develop in ACL medium and regulate mechanisms precisely for stem cell self-renewal have remained largely elusive.

Our findings demonstrate that ACL-ESCs and ACL-XEN cells are derived from one blastocyst, and retain a global transcriptome signature of inner cell mass and PrE of blastocyst respectively. Accordingly, ACL-ESCs express key factors specific to naïve pluripotency and also efficiently contribute to chimeric development as well as germline transmission that is characteristic of naïve pluripotency. ACL-XEN cells are marked by primitive endoderm specific markers such as *Gata4*, *Gata6*, and *Sox17*, and chimerism experiment also provide direct evidence for the contribution of embryonic endoderm in E6.5 embryos. Such a defined culture condition ACL allow us to re-establish and research the coordinated interactions of the ESCs, TSCs and XEN cells from one blastocyst, which have remained inaccessible until now.

Recent reports showed blastoids represent an accessible, scalable, and tractable model system that will be valuable for many applications in basic research and translational approaches [24, 27–30, 75, 76]. The blastoids were generated from three different stem cells (ESCs, TSCs and XEN cells) with highly efficiency and developed to gustrulate-like stage [25, 26]. These three types stem cells are originated from blastocysts, depend on different signaling pathway regulator in *in vitro* culture condition [73]. We know, natural blastocysts develop in the environment of oviducts or uterus, and three linages always exist in same developing environment. The findings in this study demonstrated distinct two types stem cell lines were able to be derived from one blastocyst, and also be reconstructed into blastoids in same culture condition.

We demonstrate here that ACL-ESCs and ACL-XEN cells can be reconstituted to blastocyst-like structures which recapitulate early embryonic developmental processes and initiate early implantation events. Although we successfully generated ACL-blastoids from ACL-ESCs and ACL-XEN cells aggregation, most of three lineage markers were lower than natural blastocyst, especially TE lineages, and consistent with previous report that TE marker is lower in stem cell derived embryonic model [83]. Nodal/Activin signaling is required for TSCs renewal in culture and blastoids induction in previous reports [84–86]. Due to our culture conditions contain Activin A, we hypothesized that the ACL-ESCs aggregating with ACL-XEN cells might initiate TSCs differentiation and form blastocyst-like structures. In addition, we try to generated blastoids by aggregating with 2i/L-ESCs and ACL-XEN cells in ACL medium, and failed to obtain TE marker CDX2 positive cells. The result shows that ACL-ESCs is necessary for ACL-blastoid formation, and development of CDX2 positive cells relies on interaction between the ACL-ESCs and ACL-XEN cells, however, ACL-ESCs directly differentiated to TE cells, or its push ACL-XEN cell to reversed to TE cells still unclear, need further exploration.

WNT signaling pathways is active in the blastocysts and post-implantation embryos, which correlate with the formation of the blastocoel fluid-filled cavity [24, 47, 87]. To compare Activin/Nodal and STAT3/LIF signaling, our result shows WNT signaling plays a key role on ACL-blastoid generation, consistent with the result of previous reported [24]. When addition of WNT inhibitor XAV939 in ACL medium (removed off CHIR) under process of generation ACL-blastoid, we failed to observed the normal blastoids formation. How does WNT pathway stimulation increased cavitation and blastoid formation needs to be solved in next step.

Here, we describe the modified cell culture system to generate two types of stem cell lines from one blastocyst and then use them to reconstruct ACL-blastoids with many similarities to blastocysts at morphological, developmental, molecular, and functional levels, although imperfect and perhaps less neatly regulated than the natural embryos. We anticipate that simple way to derived two types of stem cells from one blastocyst and to generated ACL-blastoids, support to captures mechanism of embryo lineage segregation.

Materials And Methods

Animals

Oct4-DPE-GFP (GOF/GFP) transgenic mice [88] used in this study were strain here with a mixed background of MF1, 129/sv, and C57BL/6J. Sterile-male bred, pseudopregnant, mice for production of chimeras were strain from CD1 (ICR).

Derivation of ACL-ESCs

Mouse blastocysts (E3.5) were isolated from 129/sv females mated with males carrying GOF/GFP transgenic whose green fluorescence indicated expression in the ICM of blastocysts, PGC in vivo as well as in ESCs [88]. Blastocysts were collected at the relevant stages from the uterus in M2 medium (Sigma-Aldrich). Zona pellucida were then removed by Acidic Tyrode's Solution, Acid (Sigma-Aldrich) and blastocysts were washed with M2 for three times. Subsequently, they were placed in 24-well fibronectin-coated (16.7 μg/mL, Millipore) plate with ACL medium consisting of N2B27 medium supplemented with Activin A (20 ng/mL, R&D Systems), CHIR9902 (3 μM, Miltenyi Biotech) as well as leukemia inhibitory factor (1000 IU/mL, Millipore). N2B27 medium was used as basic medium including 1:1 mixture of DMEM/F12 medium (Gibco) and neurobasal medium (Gibco), 0.5% N2 (Gibco), 1% B27 (Gibco), 1% Glutamax (Gibco), 1% NEAA (Gibco), 100 μM β-mercaptoethanol (Sigma), and 1% penicillin/streptomycin (Gibco). Within following 3 ~ 5days, most of blastocysts attached and then formed heterogeneous outgrowths which were domed and GOF-GFP positive in the middle, while the "flat" epithelial-like and GOF-GFP negative cells were surrounding in a radial flow. On the 9th day, when the diameter of GOF-GFP positive clone grew to around 200 μm, it was picked, followed by cutting into small pieces with glass needle for 2–3 passages and dissociating with Accutase (Gibco), then forming domed GOF-GFP positive clones resembling 2i/L-ESCs in morphology. Here, we designated these cells as ACL-ESCs.

Derivation of ACL-XEN cells

The "flat" and GOF-GFP negative outgrowths spreading out on 10th day was disaggregated into single cells with TrypLE (Gibco) and cultured in ACL medium equally. As colonies reached 80–90% confluence, cells were passage into a 24-well fibronectin-coated plate regularly every 2–3 days. These cells, referred to as ACL-XEN cells, were capable of self-renewal for over 35 passages.

Derivation of 2iL-ESCs

E3.5 blastocysts with GOF-GFP collected from the uterus, zona pellucidae were removed using acid Tyrode's solution (Sigma-Aldrich) and placed on a 24-well coated by fibronectin (16.7 μg/mL, Millipore) at least 0.5 h before use. Serum-free ESC culture medium (2i/LIF) was prepared as previously described [6]. Briefly, N2B27 basic medium was supplemented with PD0325901 (PD, 1 μM, Miltenyi Biotech), CHIR99021 (CH, 3 μM, Miltenyi Biotech) and leukemia inhibitory factor (LIF, 1000 IU/mL, Millipore), which henceforth were called 2i/L-medium. Within 5–6 days, ICM of blastocysts cultures grew efficiently and outgrowth was formed. When colonies grew to around 200 μm in diameter, they were picked and minced into pieces by glass needles, then cultured in 2i/L-medium. Colonies were passaged manually for 2–3

passages as above and then treated with Accutase (Gibco) regularly every 2 days. These cells were designed as 2iL-ESCs.

Derivation of XEN cell lines

To derive XEN cell lines, a previous protocol [13] with modifications was followed. E3.5 embryos with CD1 (ICR) background were placed in Tyrode's solution (Sigma-Aldrich) to remove the zona pellucida and washed in M2 (Sigma-Aldrich) for three times, then were transferred into XEN cells derivation medium (30% TS medium and 70% Feeder-conditioned medium from mouse embryonic fibroblasts) without any growth factors. The plates were all pre-treated with fibronectin 0.5 hour (h) before use. The blastocyst attached and formed outgrowth in 3–5 days culture, while medium was changed every 3 days. At day 9–12, the spreading outgrowth was disaggregated into single cells with TrypLE for 7 min and dissociation was stopped with XEN cells derivation medium. The cell pellets were resuspended and seeded onto 24-well plates pre-treated with fibronectin. After 2–3 passages with high confluence, XEN cells were growing efficiently.

Immunofluorescence (IF) staining

Immunofluorescence for 2D (Dimensions) cell culture, ACL-blastoids, early mouse embryos, chimeric embryos, and post-implantation embryo-like structures was carried out as follow: the samples were briefly washed in DPBS (Gibco) and then fixed with freshly prepared 4% para formaldehyde (Solarbio) in DPBS for 15 min at room temperature. Subsequently, the samples were permeabilized for 30 min with 1% BSA (Gibco) and 0.1% Triton X-100 (Sigma) in DPBS, then were incubated with primary antibodies diluted in the buffer described above at 4°C overnight. After 5 min per wash for three times with 1% BSA and 0.1% Triton X-100 in DPBS, samples were incubated with fluorescence-conjugated secondary antibodies diluted in the above buffer for 1 h (2D cell culture, ACL-blastoids, chimeric embryos, and early mouse embryos) or overnight (post-implantation embryo-like structures) at room temperature in the dark. Then samples were mounted in Vectashield with DAPI (Vector Laboratories) after once washing with DPBS containing 1% BSA and 0.1% Triton X-100 and twice with DPBS. Image acquisition was performed using Nikon confocal microscope (Nikon, Tokyo, Japan) or Zeiss LSM 710 confocal microscope. The primary antibodies and dilutions used were : mouse monoclonal OCT4 (BD Biosciences, 1:200), rat monoclonal NANOG (eBioscience, 1:500), goat polyclonal SOX2 (Santa Cruz, 1:200), rat monoclonal E-Cadherin (Takara, 1:200), goat polyclonal GATA4 (R&D Systems, 1:100), goat polyclonal GATA6 (R&D Systems, 1:100), goat polyclonal SOX17 (R&D Systems, 1:200), mouse monoclonal CDX2 (Biogenex, 1:200), rabbit monoclonal YAP (Abcam, 1:500), rabbit polyclonal N-Cadherin (Abcam, Cambridge, 1:200), rat polyclonal Podocalyxin (PCX) (R&D Systems, 1:500). All secondary antibodies used were Alexa Fluor 488 or Alexa Fluor 568 (Molecular Probes, Eugene, CA, USA) highly cross-adsorbed.

Production of chimeras from ACL-ESCs / ACL-XEN cells

Using a piezo-assisted micromanipulator attached to an inverted microscope, approximately, 8–12 ACL-ESCs were injected into eight-cell stage embryos collected from E2.5 CD1 (ICR) mice recipient, which were then cultured in KSOM medium (Millipore) overnight at 37°C in a 5% CO2 atmosphere to obtain chimeric

blastocysts. After re-expansion of the blastocoel cavity, part of chimeric blastocysts was transferred to uteri of pseudopregnant CD1 (ICR) mice at 2.5 days post coitus (dpc) to generate chimeras and the remaining chimeric blastocysts continued to be cultured for another 24h, which were fixed in 4% paraformaldehyde for Immunofluorescence. By the coat color pattern of the pups at birth, full-term chimeras were able to be confirmed.

To generate chimeric embryos of ACL-XEN cells, 8–12 cells were gently injected into perivitelline space of eight-cell stage embryos. For 48h culturing in KSOM medium at 37°C in a 5% CO2 atmosphere, chimeric embryos were hatched and then fixed for IF. E6.5 CD1 (ICR) mice wild type gastrulae were also collected, then ACL-XEN cells were microinjected into the cavity of gastrulae, which were cultured in ACL medium for 48h to trace the ACL-XEN cells.

Generation of ACL-blastoids

Incubation with Accutase and TrypLE ACL-ESCs with GOF-GFP and ACL-XEN cells with tdTomato were respectively dissociated into single cells, which were then mixed as a proportion of 1:5 with a total concentration of 1×10^5 cells/mL. Then, by centrifugation for 3 min at 1300 rpm, cell pellet was resuspended with 800 μL ACL-blastoids medium and then transferred into one well of 24-well plate being coated by Anti-Adherence Rinsing Solution (StemCell Technologies) at least 0.5 h before use, which was as the day 0 of whole aggregation process. ACL-blastoids medium contained 50% N2B27 medium and 50% KSOM medium as basic medium supplemented with Activin A (20 ng/mL, R&D Systems), CHIR9902 (3 μM, Miltenyi Biotech) as well as LIF (1000 IU/mL, Millipore). From the 2nd day, 400 μL of supernatant were carefully replaced with fresh medium every two days. In the first two days, there was not any cavity formation but small aggregates. ACL-blastoids emergence was able to be observed at day 3 after cell seeding and ACL-blastoids continued to enlarge, reaching a normal size resembling E3.5 blastocyst around day 5, which were picked up with mouth pipette and fixed for IF or RNA extraction.

Culturing of ACL-blastoids by inhibitor treatments or other aggregates

A total concentration of 1×10^5 cells/mL were mixed with ACL-ESCs and ACL-XEN cells as a proportion of 1:5 (for aggregates with other cell lines, ACL-ESCs was replaced with ESCs or ACL-XEN cells was replaced with XEN cells). Cell pellet was transfered into a 24-well plate pre-coated by Anti-Adherence Rinsing Solution, and suspended with inhibitor treatments ACL-blastoids medium or ETX medium. Other aggregates were all cultured with ACL-blastoids medium. Fresh medium was added after discarding 400 μL supernatant every 2 days since aggregation. Inhibitor treatments ACL-blastoids medium was prepared with ACL-blastoids basic medium supplemented with SB431542 (10 μM, R&D Systems), CHIR9902 (3 μM, Miltenyi Biotech) and LIF (1000 IU/mL, Millipore) as A (-) treatments ACL-blastoids medium. C (-) treatments ACL-blastoids medium was based on ACL-blastoids basic medium containing Activin A (20 ng/mL, R&D Systems), XAV 939 (10 μM, R&D Systems) and LIF (1000 IU/mL, Millipore), and L (-) treatments ACL-blastoids medium was supplemented with Activin A (20 ng/mL, R&D Systems), CHIR99021 (3 μM, Miltenyi Biotech) as well as Jak inhibitor I (0.6 μM, Calbiochem). ETX medium used in

this study [25] includes 39% advanced RPMI 1640 (Gibco) and 39% DMEM (Gibco) supplement with 17.5% FBS (Gibco), 2 mM GlutaMAX (Gibco), 0.1 mM 2-mercaptoethanol (Sigma), 0.1 mM MEM nonessential amino acids (Gibco), 1 mM sodium pyruvate (Gibco), 1% penicillin-streptomycin (Gibco). Changed medium with 2 mL fresh reconstructed embryo medium every day.

Derivation of three types of stem cells from ACL-blastoids

For ESCs derivation, individual ACL-blastoid was transferred onto a fibronectin-coated 24-well plate and cultured with 2i/L-medium, which consisted of N2B27 basic medium with PD0325901 (1 μM, Miltenyi Biotec), CHIR99021 (3 μM, Miltenyi Biotec) and LIF (1000 IU/mL, Millipore). Within 3–4 days, ACL-blastoids attached and then formed outgrowths. As individual colony grew to around 200 μm in diameter, they were minced into pieces and transferred into a new 24-well plate with fibronectin pre-treatment. Then the colonies grown for 3–4 days were treated with Accutase for cell line derivation.

To derive TS cells, ACL-blastoid were transferred to one well of 24-well plate with a layer of irradiated MEF feeders [7] and outgrowth was observed within 3–4 days. At day 6–7, outgrowth was picked up and dissociated with 0.05% trypsin-EDTA (Biological industries) and plated into a new 24-well plate with MEF feeders. TS cells were cultured in TSC basal medium composed of RPMI 1640 (Gibco) supplemented with 20% Fetal Bovine Serum (FBS) (Gibco), 1X GlutaMAX (Gibco), 1X Sodium pyruvate (Gibco), and 0.1 mM 2-mercaptoethanol (Sigma), then added with 25 ng/mL rhFGF4 (R&D Systems) and 1 μg/mL Heparin (Sigma-Aldrich).

XEN cell lines were established following protocol [13] with modifications. ACL-blastois were plated individually in a 24-well plate pre-coated with fibronectin in XEN derivation medium (30% TS medium and 70% Feeder-conditioned medium from mouse embryonic fibroblasts) and supplemented with 25 ng/mL rhFGF4 and 1 mg/mL Heparin. The outgrowth was formed around day 3. In the following days, medium was changed every 3 days. At around day 10, the XEN cells were dissociated into single cells using TrypLE for 7 min at 37 C. Dissociation was stopped with 70cond medium and cells were collected by centrifugation at 1300 rpm for 3 min, then pellets were resuspended and plated into a 24-well plate pre-coated with fibronectin. FGF4 and Heparin were removed from the XEN derivation medium after 2–3 stable passages, once the XEN cells were established and growing well.

Embryos and ACL-blastoids transfer

The 2.5 dpc recipient was anesthetized with Avedine (Aibei) and the uterine horn was exposed by surgery. Chimeric embryos or ACL-blastoids at day 5 were picked up and transferred into KSOM droplets using a mouth pipette and washed for three times. Subsequently, around 10–15 chimeric embryos or ACL-blastoids were transferred to each side of uterine horn pre-punctured with a needle. At 6.5 or 7.5 dpc, postimplantation embryo-like structures were collected from deciduae at implantation sites in the uterus dissected out.

Karyotype

Both of ACL-ESCs and ACL-XEN cells were prepared for cytogenetic analysis by treatment with colchicine (Sigma) at a final concentration of 0.2 μg/mL for 2.5 h to accumulate cells in metaphase. Following harvest of cells, the cell pellets were exposed to 8 mL 0.075M KCl (Sigma) for 10 min at 37°C for hypotonic treatment and cold fixative solution prepared with 3:1 methanol : acetic acid of 1 mL was gently added and mixed. After discarding the supernatant, cells were fixed for 3 times at 37°C with 8 mL fixative solution for 30 min each time. Then, cells were suspended with 0.5 mL cold fixative solution and dropped onto pre-cold clean slides, which were dried for 1h at 70°C in an incubator. After cooling down at room temperature, the slides were stained with Giemsa (Sigma) for 10 min and unfixed dyes were washed off with distilled water. The slides were photographed with a microscope (Nikon, Tokyo, Japan), and the preparations were analyzed by LUCIA Cytogenetics (Lucia, Praha, Czech Republic).

RT-qPCR

Total RNA of cultured cells was extracted with a RNeasy Mini Kit (Qiagen). ACL-blastoids or nature blastocysts was isolated and purified using PicoPure™ RNA Isolation Kit (Thermo Fisher) following the manufacturer's instructions. Complementary DNA (cDNA) was synthesized using the Reverse Transcription System (Promega). Real-time quantitative polymerase chain reactions (RT-qPCR) were set up using the SYBR FAST Universal qPCR kit (KAPA) and were performed on LightCycler 96 Instrument II (Roche Life Science). Each experiment was carried out with technical triplicates. Primer pairs are listed in Supplementary Table 1.

RNA extraction and sequencing

Total RNA were extracted from approximately 2×10^6 cells using an RNeasy Mini Kit (QIAGEN) according to the recommendations of manufacturer and then an NEBNext Poly(A) mRNA Magnetic Isolation Module was used to isolate mRNA from total RNA. Using mRNA as input, the first- and second-strand cDNAs were synthesized using the NEBNext RNA First Strand Synthesis Module and the NEBNext Ultra II Non-Directional RNA Second Strand Synthesis Module, respectively. Final libraries were prepared using KAPA Hyper Prep Kits (eight PCR cycles) and sequenced on a HiSeq 4000 platform.

RNA-seq and analysis

Before alignment, raw data were first trimmed to remove reads with more than 10% low-quality bases and to trim adaptors. Then the clean reads were mapped to mouse reference genome (mm10) with TopHat (2.0.12) with default settings [89]. HTSeq (0.6.1) was used for reads counting, and then RefSeq gene expression level was estimated using the RPKM method (reads per kilobase transcriptome per million reads). In vivo data of mouse embryos E4.5 PrE [66] and ESCs (GSE119985) [60] from a previous study were downloaded and identically processed. DEGs in different samples were determined using the edgeR package with fold change R 2 and p % 0.5 [90]. UHC analysis was performed by the R *hclust* function. t-SNE was carried out with the R *Rtsne* function. Heatmaps of select genes were performed using the R *heatmap.2* function. Principal component analysis was performed with the R *prcomp* function. GO analysis was performed using Metascape (http://metascape.org). Trend analysis of DEGs was performed using Short Time-series Expression Miner software [67].

Statistical analyses

Statistical analyses were performed with the GraphPad Prism software (v8.0.2). Data were represented as mean ± SD. Significance between each group was measured by unpaired two-tailed Student's *t* test and a value of $p < 0.05$ was considered statistically significant.

Declarations

DATA AVAILABILITY

RNA-seq data was deposited in the Genome Sequence Archive (GSA) under accession number CRA005808. All data that support the conclusions in the study are available from the authors on reasonable request.

ACKNOWLEDGMENTS

We thank the sequencing platform and bioinformation analysis of Gene Denovo Biotechnology Co., Ltd (Guangzhou, China). This work was supported by grants from the National Natural Science Foundation of China (32060176), the Program of Higher-Level Talents of Inner Mongolia University (10000-21311201/058), the Inner Mongolia Autonomous Region Science and Technology Plan of China (2020ZD0007), the Inner Mongolia Autonomous Region Natural Science Foundation (2021MS03003).

AUTHOR CONTRIBUTIONS

B.W., X.L., and S.B. conceived the research project. B.W. and Y.Z. derived ACL-ESCs / ACL-XEN cells and performed in vivo embryo experiment. Y.Z. generated and analyzed molecular properties of ACL-blastoids under the supervision of B.W. and S.B. Z.Y., Y.L., J.L., and C.C. analyzed molecular properties of ACL-ESCs / ACL-XEN cells. B.W., Z.Y., and S.B. wrote the manuscript with input from all authors.

COMPETING INTERESTS

The authors declare that they have no competing interests.

ETHICS APPROVAL AND CONSENT TO PARTICIPATE

All animal experiments were carried out with humane methods in compliance with animal ethical standards approved by Animal Research Committee of Inner Mongolia University, China.

References

1. Arnold SJ, Robertson EJ. Making a commitment: cell lineage allocation and axis patterning in the early mouse embryo. Nature reviews Molecular cell biology, **10** 91–103(2009).

2. Rossant J, Tam PP. Blastocyst lineage formation, early embryonic asymmetries and axis patterning in the mouse. Development (Cambridge, England), **136** 701–13(2009).
3. Zernicka-Goetz M, Morris SA, Bruce AW. Making a firm decision: multifaceted regulation of cell fate in the early mouse embryo. Nature reviews Genetics, **10** 467–77(2009).
4. Evans MJ, Kaufman MH. Establishment in culture of pluripotential cells from mouse embryos. Nature, **292** 154–6(1981).
5. Martin GR. Isolation of a pluripotent cell line from early mouse embryos cultured in medium conditioned by teratocarcinoma stem cells. Proc Natl Acad Sci U S A, **78** 7634–8(1981).
6. Ying QL, Wray J, Nichols J, Batlle-Morera L, Doble B, Woodgett J, *et al.* The ground state of embryonic stem cell self-renewal. Nature, **453** 519–23(2008).
7. Tanaka S, Kunath T, Hadjantonakis AK, Nagy A, Rossant J. Promotion of trophoblast stem cell proliferation by FGF4. Science, **282** 2072–5(1998).
8. Kunath T, Arnaud D, Uy GD, Okamoto I, Chureau C, Yamanaka Y, *et al.* Imprinted X-inactivation in extra-embryonic endoderm cell lines from mouse blastocysts. Development (Cambridge, England), **132** 1649–61(2005).
9. Rayon T, Menchero S, Nieto A, Xenopoulos P, Crespo M, Cockburn K, *et al.* Notch and hippo converge on Cdx2 to specify the trophectoderm lineage in the mouse blastocyst. Dev Cell, **30** 410–22(2014).
10. Tam PP, Rossant J. Mouse embryonic chimeras: tools for studying mammalian development. Development (Cambridge, England), **130** 6155–63(2003).
11. Hayakawa K, Himeno E, Tanaka S, Kunath T. Isolation and manipulation of mouse trophoblast stem cells. *Current protocols in stem cell biology*, **32** 1e.4.1-e.4.32(2015).
12. Simmons DG, Fortier AL, Cross JC. Diverse subtypes and developmental origins of trophoblast giant cells in the mouse placenta. Developmental biology, **304** 567–78(2007).
13. Rugg-Gunn P. Derivation and Culture of Extra-Embryonic Endoderm Stem Cell Lines. Cold Spring Harb Protoc, **2017** (2017).
14. Niakan KK, Schrode N, Cho LT, Hadjantonakis AK. Derivation of extraembryonic endoderm stem (XEN) cells from mouse embryos and embryonic stem cells. Nat Protoc, **8** 1028–41(2013).
15. Pierce GB, Arechaga J, Muro C, Wells RS. Differentiation of ICM cells into trophectoderm. The American journal of pathology, **132** 356–64(1988).
16. Niwa H, Toyooka Y, Shimosato D, Strumpf D, Takahashi K, Yagi R, *et al.* Interaction between Oct3/4 and Cdx2 determines trophectoderm differentiation. Cell, **123** 917–29(2005).
17. Fujikura J, Yamato E, Yonemura S, Hosoda K, Masui S, Nakao K, *et al.* Differentiation of embryonic stem cells is induced by GATA factors. Genes & development, **16** 784–9(2002).
18. Shimosato D, Shiki M, Niwa H. Extra-embryonic endoderm cells derived from ES cells induced by GATA factors acquire the character of XEN cells. BMC developmental biology, **7** 80(2007).
19. Doetschman TC, Eistetter H, Katz M, Schmidt W, Kemler R. The in vitro development of blastocyst-derived embryonic stem cell lines: formation of visceral yolk sac, blood islands and myocardium.

Journal of embryology and experimental morphology, **87** 27–45(1985).

20. Anderson KGV, Hamilton WB, Roske FV, Azad A, Knudsen TE, Canham MA, *et al.* Insulin fine-tunes self-renewal pathways governing naive pluripotency and extra-embryonic endoderm. Nature cell biology, **19** 1164–77(2017).
21. Linneberg-Agerholm M, Wong YF, Romero Herrera JA, Monteiro RS, Anderson KGV, Brickman JM. Naïve human pluripotent stem cells respond to Wnt, Nodal and LIF signalling to produce expandable naïve extra-embryonic endoderm. Development (Cambridge, England), **146** (2019).
22. Cho LT, Wamaitha SE, Tsai IJ, Artus J, Sherwood RI, Pedersen RA, *et al.* Conversion from mouse embryonic to extra-embryonic endoderm stem cells reveals distinct differentiation capacities of pluripotent stem cell states. Development (Cambridge, England), **139** 2866–77(2012).
23. Burkert U, von Rüden T, Wagner EF. Early fetal hematopoietic development from in vitro differentiated embryonic stem cells. The New biologist, **3** 698–708(1991).
24. Rivron NC, Frias-Aldeguer J, Vrij EJ, Boisset JC, Korving J, Vivié J, *et al.* Blastocyst-like structures generated solely from stem cells. Nature, **557** 106–11(2018).
25. Zhang S, Chen T, Chen N, Gao D, Shi B, Kong S, *et al.* Implantation initiation of self-assembled embryo-like structures generated using three types of mouse blastocyst-derived stem cells. Nat Commun, **10** 496(2019).
26. Sozen B, Amadei G, Cox A, Wang R, Na E, Czukiewska S, *et al.* Self-assembly of embryonic and two extra-embryonic stem cell types into gastrulating embryo-like structures. Nature cell biology, **20** 979 – 89(2018).
27. Sozen B, Cox AL, De Jonghe J, Bao M, Hollfelder F, Glover DM, *et al.* Self-Organization of Mouse Stem Cells into an Extended Potential Blastoid. Dev Cell, **51** 698–712 e8(2019).
28. Li R, Zhong C, Yu Y, Liu H, Sakurai M, Yu L, *et al.* Generation of Blastocyst-like Structures from Mouse Embryonic and Adult Cell Cultures. Cell, **179** 687–702.e18(2019).
29. Yanagida A, Spindlow D, Nichols J, Dattani A, Smith A, Guo G. Naive stem cell blastocyst model captures human embryo lineage segregation. Cell stem cell, **28** 1016-22.e4(2021).
30. Yu L, Wei Y, Duan J, Schmitz DA, Sakurai M, Wang L, *et al.* Blastocyst-like structures generated from human pluripotent stem cells. Nature, **591** 620–6(2021).
31. Moris N, Anlas K, van den Brink SC, Alemany A, Schröder J, Ghimire S, *et al.* An in vitro model of early anteroposterior organization during human development. Nature, **582** 410–5(2020).
32. Beccari L, Moris N, Girgin M, Turner DA, Baillie-Johnson P, Cossy AC, *et al.* Multi-axial self-organization properties of mouse embryonic stem cells into gastruloids. Nature, **562** 272–6(2018).
33. van den Brink SC, Baillie-Johnson P, Balayo T, Hadjantonakis AK, Nowotschin S, Turner DA, *et al.* Symmetry breaking, germ layer specification and axial organisation in aggregates of mouse embryonic stem cells. Development (Cambridge, England), **141** 4231–42(2014).
34. Baillie-Johnson P, van den Brink SC, Balayo T, Turner DA, Martinez Arias A. Generation of Aggregates of Mouse Embryonic Stem Cells that Show Symmetry Breaking, Polarization and Emergent Collective

Behaviour In Vitro. Journal of visualized experiments: JoVE (2015).

35. Girgin MU, Broguiere N, Mattolini L, Lutolf MP. Gastruloids generated without exogenous Wnt activation develop anterior neural tissues. Stem cell reports, **16** 1143–55(2021).
36. van den Brink SC, Alemany A, van Batenburg V, Moris N, Blotenburg M, Vivié J, *et al.* Single-cell and spatial transcriptomics reveal somitogenesis in gastruloids. Nature, **582** 405–9(2020).
37. Veenvliet JV, Bolondi A, Kretzmer H, Haut L, Scholze-Wittler M, Schifferl D, *et al.* Mouse embryonic stem cells self-organize into trunk-like structures with neural tube and somites. Science, **370** (2020).
38. Rossi G, Broguiere N, Miyamoto M, Boni A, Guiet R, Girgin M, *et al.* Capturing Cardiogenesis in Gastruloids. Cell stem cell, **28** 230 – 40.e6(2021).
39. Turner DA, Girgin M, Alonso-Crisostomo L, Trivedi V, Baillie-Johnson P, Glodowski CR, *et al.* Anteroposterior polarity and elongation in the absence of extra-embryonic tissues and of spatially localised signalling in gastruloids: mammalian embryonic organoids. Development (Cambridge, England), **144** 3894–906(2017).
40. Papanayotou C, Collignon J. Activin/Nodal signalling before implantation: setting the stage for embryo patterning. Philosophical transactions of the Royal Society of London Series B, Biological sciences, **369** (2014).
41. Kaufman-Francis K, Goh HN, Kojima Y, Studdert JB, Jones V, Power MD, *et al.* Differential response of epiblast stem cells to Nodal and Activin signalling: a paradigm of early endoderm development in the embryo. Philosophical transactions of the Royal Society of London Series B, Biological sciences, **369** (2014).
42. Granier C, Gurchenkov V, Perea-Gomez A, Camus A, Ott S, Papanayotou C, *et al.* Nodal cis-regulatory elements reveal epiblast and primitive endoderm heterogeneity in the peri-implantation mouse embryo. Developmental biology, **349** 350 – 62(2011).
43. Kumar A, Lualdi M, Lyozin GT, Sharma P, Loncarek J, Fu XY, *et al.* Nodal signaling from the visceral endoderm is required to maintain Nodal gene expression in the epiblast and drive DVE/AVE migration. Developmental biology, **400** 1–9(2015).
44. Robertson EJ. Dose-dependent Nodal/Smad signals pattern the early mouse embryo. Seminars in cell & developmental biology, **32** 73–9(2014).
45. Brennan J, Lu CC, Norris DP, Rodriguez TA, Beddington RS, Robertson EJ. Nodal signalling in the epiblast patterns the early mouse embryo. Nature, **411** 965–9(2001).
46. Robertson EJ, Norris DP, Brennan J, Bikoff EK. Control of early anterior-posterior patterning in the mouse embryo by TGF-beta signalling. *Philosophical transactions of the Royal Society of London Series B, Biological sciences*, **358** 1351-7; discussion 7(2003).
47. Kemp C, Willems E, Abdo S, Lambiv L, Leyns L. Expression of all Wnt genes and their secreted antagonists during mouse blastocyst and postimplantation development. Developmental dynamics: an official publication of the American Association of Anatomists, **233** 1064–75(2005).
48. Martyn I, Kanno TY, Ruzo A, Siggia ED, Brivanlou AH. Self-organization of a human organizer by combined Wnt and Nodal signalling. Nature, **558** 132–5(2018).

49. Tanaka SS, Kojima Y, Yamaguchi YL, Nishinakamura R, Tam PP. Impact of WNT signaling on tissue lineage differentiation in the early mouse embryo. Development, growth & differentiation, **53** 843–56(2011).
50. Batista MR, Diniz P, Murta D, Torres A, Lopes-da-Costa L, Silva E. Balanced Notch-Wnt signaling interplay is required for mouse embryo and fetal development. Reproduction (Cambridge, England), **161** 385 – 98(2021).
51. Lloyd S, Fleming TP, Collins JE. Expression of Wnt genes during mouse preimplantation development. Gene expression patterns: GEP, **3** 309–12(2003).
52. Mohamed OA, Dufort D, Clarke HJ. Expression and estradiol regulation of Wnt genes in the mouse blastocyst identify a candidate pathway for embryo-maternal signaling at implantation. Biology of reproduction, **71** 417–24(2004).
53. Tepekoy F, Akkoyunlu G, Demir R. The role of Wnt signaling members in the uterus and embryo during pre-implantation and implantation. Journal of assisted reproduction and genetics, **32** 337–46(2015).
54. Denicol AC, Dobbs KB, McLean KM, Carambula SF, Loureiro B, Hansen PJ. Canonical WNT signaling regulates development of bovine embryos to the blastocyst stage. Scientific reports, **3** 1266(2013).
55. Sozen B, Demir N, Zernicka-Goetz M. BMP signalling is required for extra-embryonic ectoderm development during pre-to-post-implantation transition of the mouse embryo. Developmental biology, **470** 84–94(2021).
56. Bier E, De Robertis EM. EMBRYO DEVELOPMENT. BMP gradients: A paradigm for morphogen-mediated developmental patterning. Science, **348** aaa5838(2015).
57. Reyes de Mochel NS, Luong M, Chiang M, Javier AL, Luu E, Toshihiko F, *et al.* BMP signaling is required for cell cleavage in preimplantation-mouse embryos. Developmental biology, **397** 45–55(2015).
58. Morgani SM, Brickman JM. LIF supports primitive endoderm expansion during pre-implantation development. Development (Cambridge, England), **142** 3488–99(2015).
59. Do DV, Ueda J, Messerschmidt DM, Lorthongpanich C, Zhou Y, Feng B, *et al.* A genetic and developmental pathway from STAT3 to the OCT4-NANOG circuit is essential for maintenance of ICM lineages in vivo. Genes & development, **27** 1378–90(2013).
60. Wu B, Li L, Li B, Gao J, Chen Y, Wei M, *et al.* Activin A and BMP4 Signaling Expands Potency of Mouse Embryonic Stem Cells in Serum-Free Media. Stem cell reports, **14** 241 – 55(2020).
61. Saiz N, Mora-Bitria L, Rahman S, George H, Herder JP, Garcia-Ojalvo J, *et al.* Growth-factor-mediated coupling between lineage size and cell fate choice underlies robustness of mammalian development. eLife, **9** (2020).
62. Biechele S, Adissu HA, Cox BJ, Rossant J. Zygotic Porcn paternal allele deletion in mice to model human focal dermal hypoplasia. PloS one, **8** e79139(2013).
63. Haegel H, Larue L, Ohsugi M, Fedorov L, Herrenknecht K, Kemler R. Lack of beta-catenin affects mouse development at gastrulation. Development (Cambridge, England), **121** 3529–37(1995).

64. Harrison SE, Sozen B, Christodoulou N, Kyprianou C, Zernicka-Goetz M. Assembly of embryonic and extraembryonic stem cells to mimic embryogenesis in vitro. Science, **356** (2017).
65. Hyun I, Wilkerson A, Johnston J. Embryology policy: Revisit the 14-day rule. Nature, **533** 169–71(2016).
66. Boroviak T, Loos R, Lombard P, Okahara J, Behr R, Sasaki E, *et al.* Lineage-Specific Profiling Delineates the Emergence and Progression of Naive Pluripotency in Mammalian Embryogenesis. Dev Cell, **35** 366–82(2015).
67. Ernst J, Bar-Joseph Z. STEM: a tool for the analysis of short time series gene expression data. BMC bioinformatics, **7** 191(2006).
68. Raina D, Bahadori A, Stanoev A, Protzek M, Koseska A, Schröter C. Cell-cell communication through FGF4 generates and maintains robust proportions of differentiated cell types in embryonic stem cells. Development (Cambridge, England), **148** (2021).
69. Kaneko KJ, DePamphilis ML. TEAD4 establishes the energy homeostasis essential for blastocoel formation. Development (Cambridge, England), **140** 3680–90(2013).
70. Nishioka N, Inoue K, Adachi K, Kiyonari H, Ota M, Ralston A, *et al.* The Hippo signaling pathway components Lats and Yap pattern Tead4 activity to distinguish mouse trophectoderm from inner cell mass. Dev Cell, **16** 398–410(2009).
71. Posfai E, Petropoulos S, de Barros FRO, Schell JP, Jurisica I, Sandberg R, *et al.* Position- and Hippo signaling-dependent plasticity during lineage segregation in the early mouse embryo. eLife, **6** (2017).
72. Yagi R, Kohn MJ, Karavanova I, Kaneko KJ, Vullhorst D, DePamphilis ML, *et al.* Transcription factor TEAD4 specifies the trophectoderm lineage at the beginning of mammalian development. Development (Cambridge, England), **134** 3827–36(2007).
73. Niwa H. How is pluripotency determined and maintained? *Development (Cambridge, England)*, **134** 635 – 46(2007).
74. Bedzhov I, Zernicka-Goetz M. Self-organizing properties of mouse pluripotent cells initiate morphogenesis upon implantation. Cell, **156** 1032–44(2014).
75. Kime C, Kiyonari H, Ohtsuka S, Kohbayashi E, Asahi M, Yamanaka S, *et al.* Induced 2C Expression and Implantation-Competent Blastocyst-like Cysts from Primed Pluripotent Stem Cells. Stem cell reports, **13** 485 – 98(2019).
76. Sozen B, Jorgensen V, Weatherbee BAT, Chen S, Zhu M, Zernicka-Goetz M. Reconstructing aspects of human embryogenesis with pluripotent stem cells. Nat Commun, **12** 5550(2021).
77. Brons IG, Smithers LE, Trotter MW, Rugg-Gunn P, Sun B, Chuva de Sousa Lopes SM, *et al.* Derivation of pluripotent epiblast stem cells from mammalian embryos. *Nature*, **448** 191-5(2007).
78. Tesar PJ, Chenoweth JG, Brook FA, Davies TJ, Evans EP, Mack DL, *et al.* New cell lines from mouse epiblast share defining features with human embryonic stem cells. Nature, **448** 196–9(2007).
79. Choi J, Huebner AJ, Clement K, Walsh RM, Savol A, Lin K, *et al.* Prolonged Mek1/2 suppression impairs the developmental potential of embryonic stem cells. Nature, **548** 219–23(2017).

80. Smith AG, Heath JK, Donaldson DD, Wong GG, Moreau J, Stahl M, *et al.* Inhibition of pluripotential embryonic stem cell differentiation by purified polypeptides. Nature, **336** 688–90(1988).
81. Williams RL, Hilton DJ, Pease S, Willson TA, Stewart CL, Gearing DP, *et al.* Myeloid leukaemia inhibitory factor maintains the developmental potential of embryonic stem cells. Nature, **336** 684–7(1988).
82. Wu B, Li Y, Li B, Zhang B, Wang Y, Li L, *et al.* DNMTs Play an Important Role in Maintaining the Pluripotency of Leukemia Inhibitory Factor-Dependent Embryonic Stem Cells. Stem cell reports, **16** 582 – 96(2021).
83. Zhao C, Reyes AP, Schell JP, Weltner J, Ortega NM, Zheng Y, *et al.* Reprogrammed blastoids contain amnion-like cells but not trophectoderm. 2021.05.07.442980(2021).
84. Guzman-Ayala M, Ben-Haim N, Beck S, Constam DB. Nodal protein processing and fibroblast growth factor 4 synergize to maintain a trophoblast stem cell microenvironment. Proc Natl Acad Sci U S A, **101** 15656–60(2004).
85. Ohinata Y, Tsukiyama T. Establishment of trophoblast stem cells under defined culture conditions in mice. PLoS One, **9** e107308(2014).
86. Kubaczka C, Senner C, Arauzo-Bravo MJ, Sharma N, Kuckenberg P, Becker A, *et al.* Derivation and maintenance of murine trophoblast stem cells under defined conditions. Stem Cell Reports, **2** 232–42(2014).
87. Yoney A, Etoc F, Ruzo A, Carroll T, Metzger JJ, Martyn I, *et al.* WNT signaling memory is required for ACTIVIN to function as a morphogen in human gastruloids. Elife, **7** (2018).
88. Yoshimizu T, Sugiyama N, De Felice M, Yeom YI, Ohbo K, Masuko K, *et al.* Germline-specific expression of the Oct-4/green fluorescent protein (GFP) transgene in mice. Development, growth & differentiation, **41** 675 – 84(1999).
89. Trapnell C, Pachter L, Salzberg SL. TopHat: discovering splice junctions with RNA-Seq. Bioinformatics (Oxford, England), **25** 1105–11(2009).
90. Robinson MD, McCarthy DJ, Smyth GK. edgeR: a Bioconductor package for differential expression analysis of digital gene expression data. Bioinformatics (Oxford, England), **26** 139–40(2010).

Figures

Fig. 1

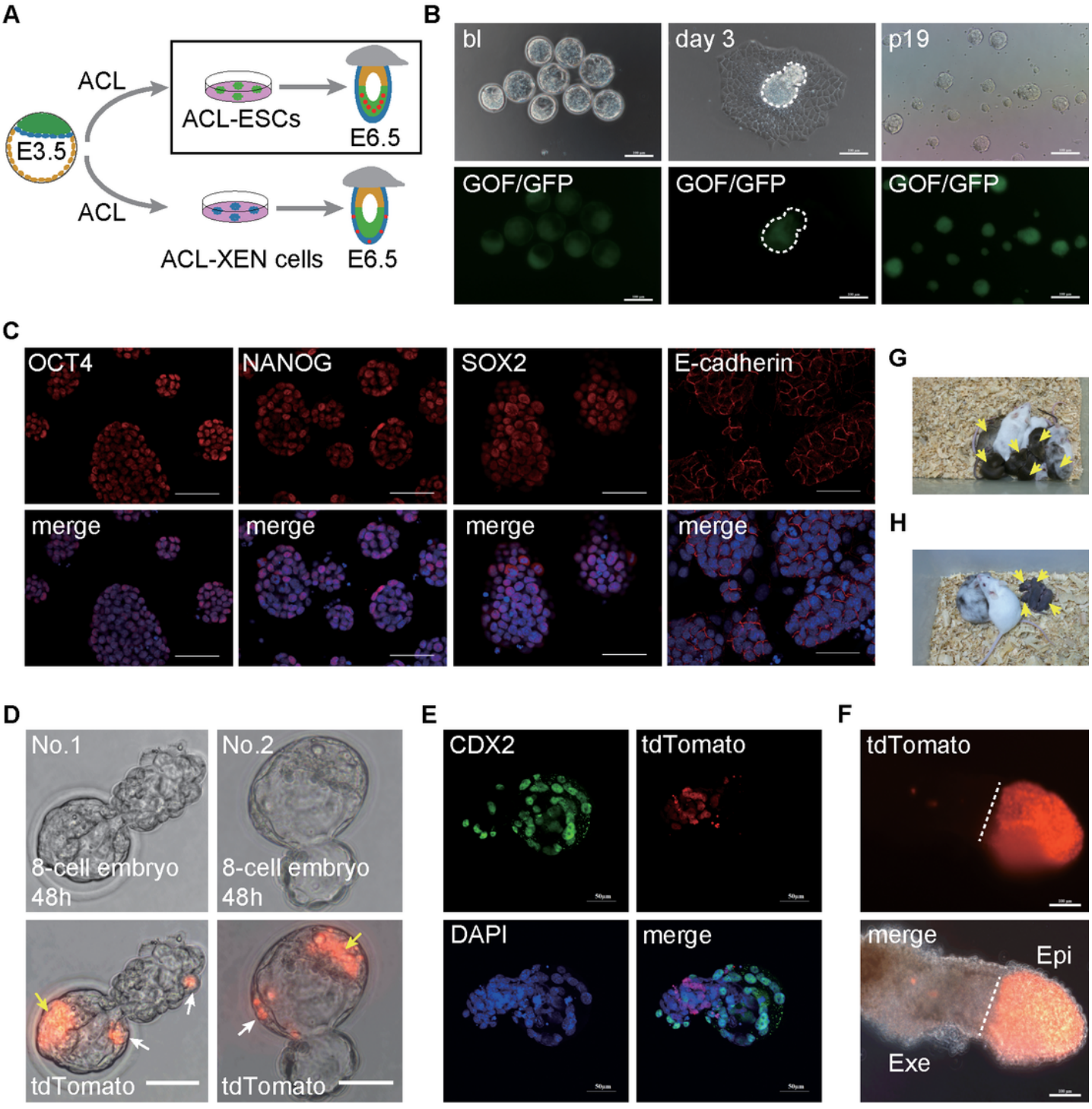

Figure 1

Activin A replaces MEK inhibitor to support ESCs pluripotency.

A Schematic of ACL-ESCs derivation from E3.5 blastocysts.

B Derivation of ACL-ESCs lines from blastocysts. bl, blastocyst. Scale bars, 100 μm.

C IF staining assays of OCT4, SOX2, and NANOG in ACL-ESCs. DAPI stained the nucleus. Scale bars, 50 μm.

D Localization of ACL-ESCs (tdTomato+) in ICM contribution (yellow arrows) and trophectoderm contribution (white arrows) in chimeric embryos *in vitro* cultured for 48 h. Scale bars, 50 μm.

E The 30 E4.5 blastocysts (hatching) developing from 8-cell stage embryos injected with ACL-ESCs were stained for CDX2 (green), which indicated no merge with H2B tdTomato+ donor cells. DAPI stained the nucleus. Scale bars, 50 μm.

F E6.5 chimeras generated by ACL-ESCs (tdTomato+). Scale bars, 100 μm. Exe, extra-embryonic ectoderm; Epi, epiblast.

G Chimeric pups (yellow arrows) generated by injecting ACL-ESCs into ICR host blastocysts (n = 3 independent experiments).

H F1 Pups (yellow arrows) generated by ACL-ESCs derived Chimera male mated with ICR female.

Fig. 2

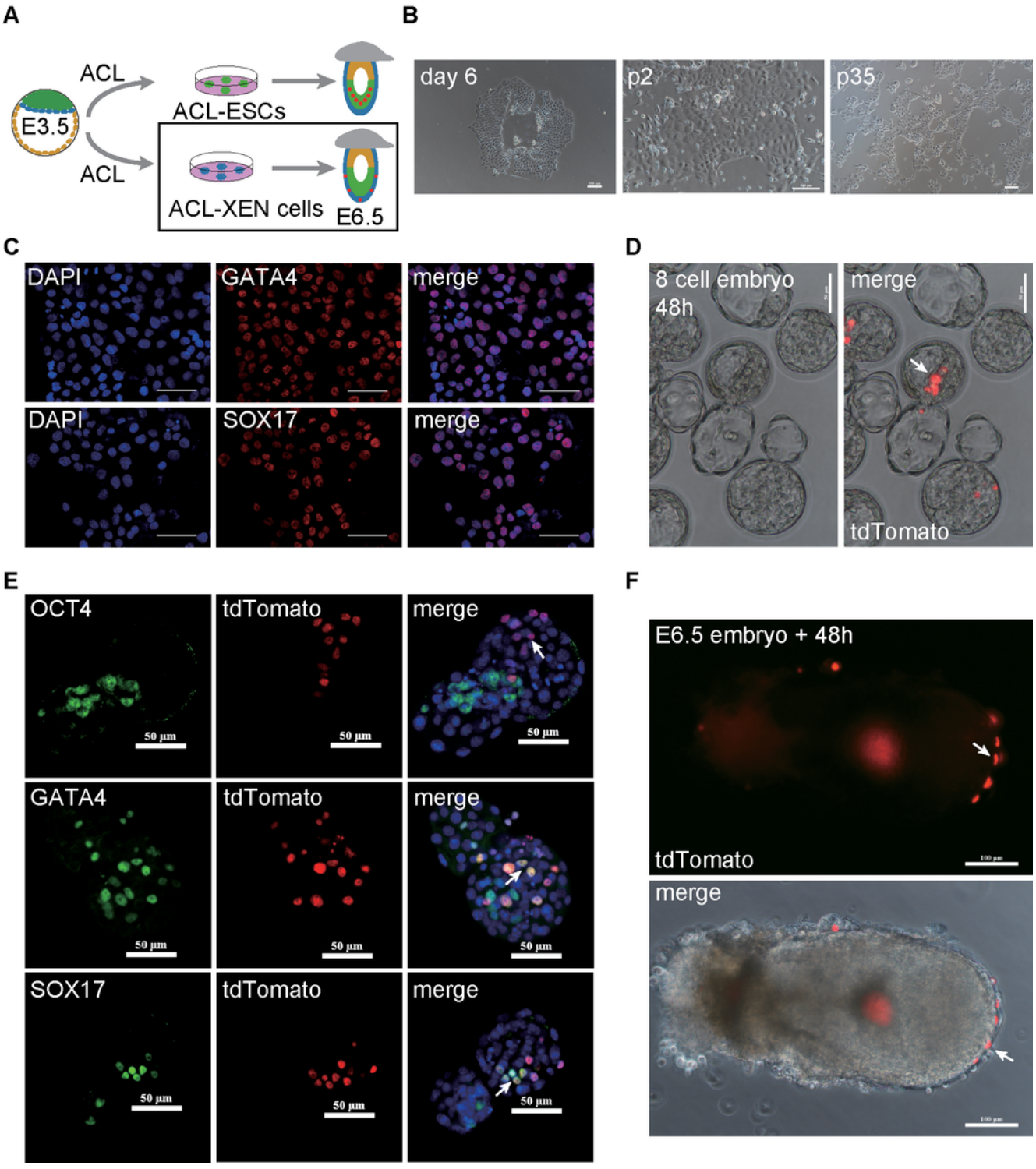

Figure 2

ACL supports XEN Cells derivation from blastocyst.

A Schematic of ACL-XEN cells derivation from E3.5 blastocyst.

B Representative images of derivation of ACL-XEN cells at day 6, and treated with TrypLE for passage 2 (p2) and passage 25 (p25). Scale bars, 100 μm.

C IF staining assays of GATA4 and SOX17 in ACL-XEN cells. DAPI stained the nucleus. Scale bars, 50 μm.

D Bright-filed images of E4.5 embryos generated after 8-cell stage embryos injection of ACL-XEN cells (tdTomato+) and cultured for 48 h *in vitro*. ACL-XEN cells (tdTomato+) in primitive endoderm (write arrow). Scale bars, 50 μm.

E IF staining of OCT4, GATA4 and SOX17 (green) of E4.5 embryos (n=30) generated after 8-cell stage embryos injection of ACL-XEN cells (tdTomato+) and cultured for 48 h *in vitro*. Arrows indicate ACL-XEN cells contribute to PrE. DAPI stained the nucleus. Scale bars, 50 μm.

F Bright filed and fluorescent images of E6.5 embryos cultured for 48 h *in vitro*, after ACL-XEN cells (tdTomato+) injected. Arrows indicate H2B tdTomato+ cells in the Visceral endoderm. Scale bars, 50 μm.

Fig. 3

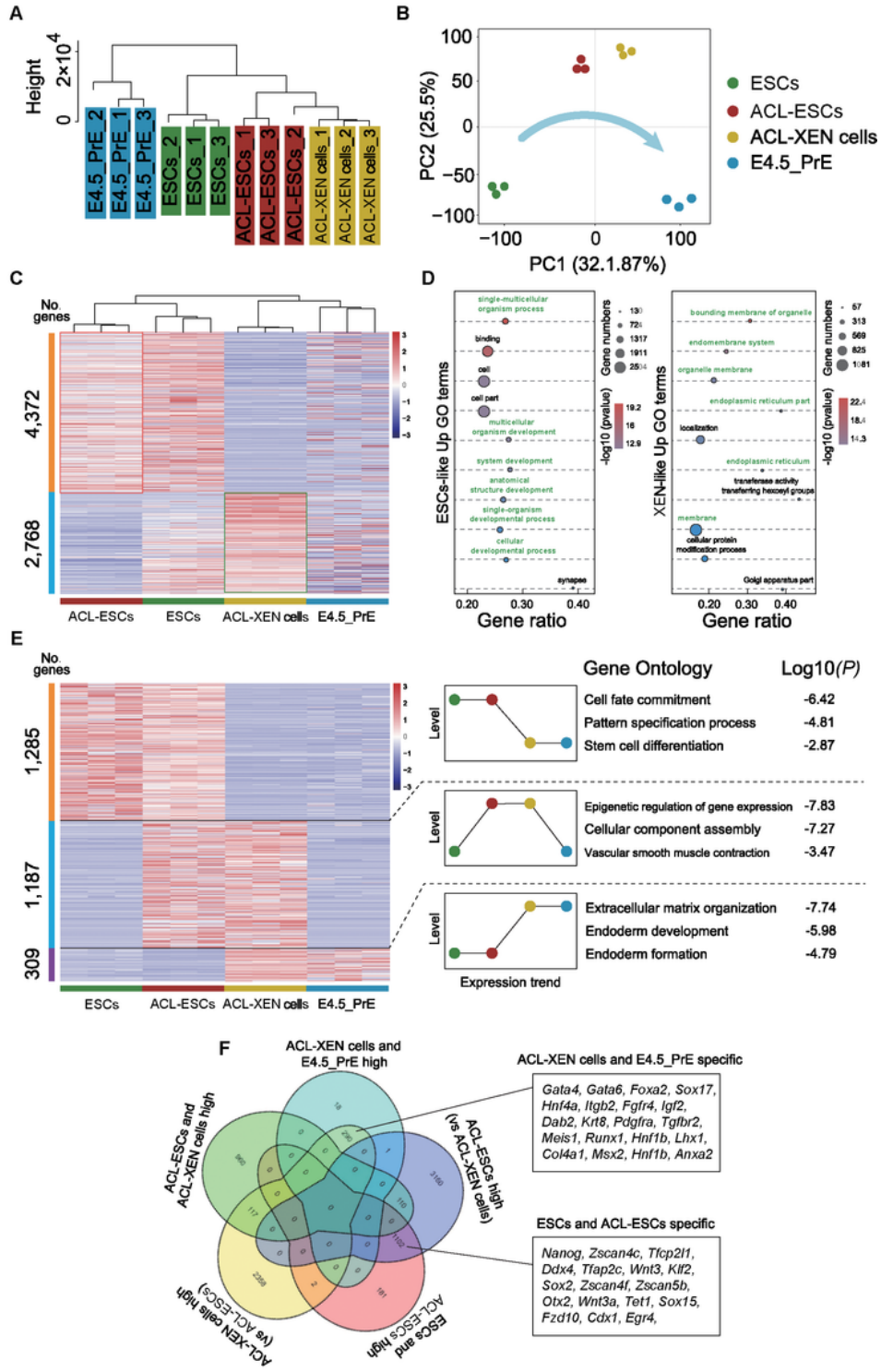

Figure 3

Analyses of molecular features of ACL-ESCs and ACL-XEN cells.

A Unsupervised hierarchical clustering (UHC) of whole-genome transcriptome on three biological replicates of three types of stem cell lines and E4.5_PrE (primitive endoderm).

B t-SNE analysis of gene expression of three types of stem cell lines and E4.5_PrE. Arrow indicates that ACL-ESCs and ACL-XEN are developmentally intermediate between ESCs and E4.5_PrE.

C Heatmap showing scaled expression values of a total of 7,140 differentially expressed genes (mean log2(normalized read counts) > 2, log2(fold change) > 2, adjusted p value < 0.05) in ACL-ESCs and ACL-XEN cells, and compared with ESCs and E4.5_PrE.

D The top representative GO terms (biological process) for ACL-ESCs and ACL-XEN cells upregulated genes.

E Comparison of ACL-ESCs, ACL-XEN cells, ESCs and E4.5_PrE. Among differentially expressed genes, a total of 1,285 genes (top) were significantly highly expressed in ACL-ESCs and ESCs compared with ACL-XEN cells and E4.5_PrE; a total of 1,187 genes (middle) were significantly upregulated in ACL-ESCs and ACL-XEN cells compared with ESCs and E4.5_PrE; a total of 309 genes (bottom) were significantly upregulated in ACL-XEN cells and E4.5_PrE compared with ESCs and ACL-XEN cells (n = 3 biological replicates on four groups).

F Venn diagram showing overlap of specific genes among ACL-ESCs, ACL-XEN cells, ESCs and E4.5_PrE.

Fig. 4

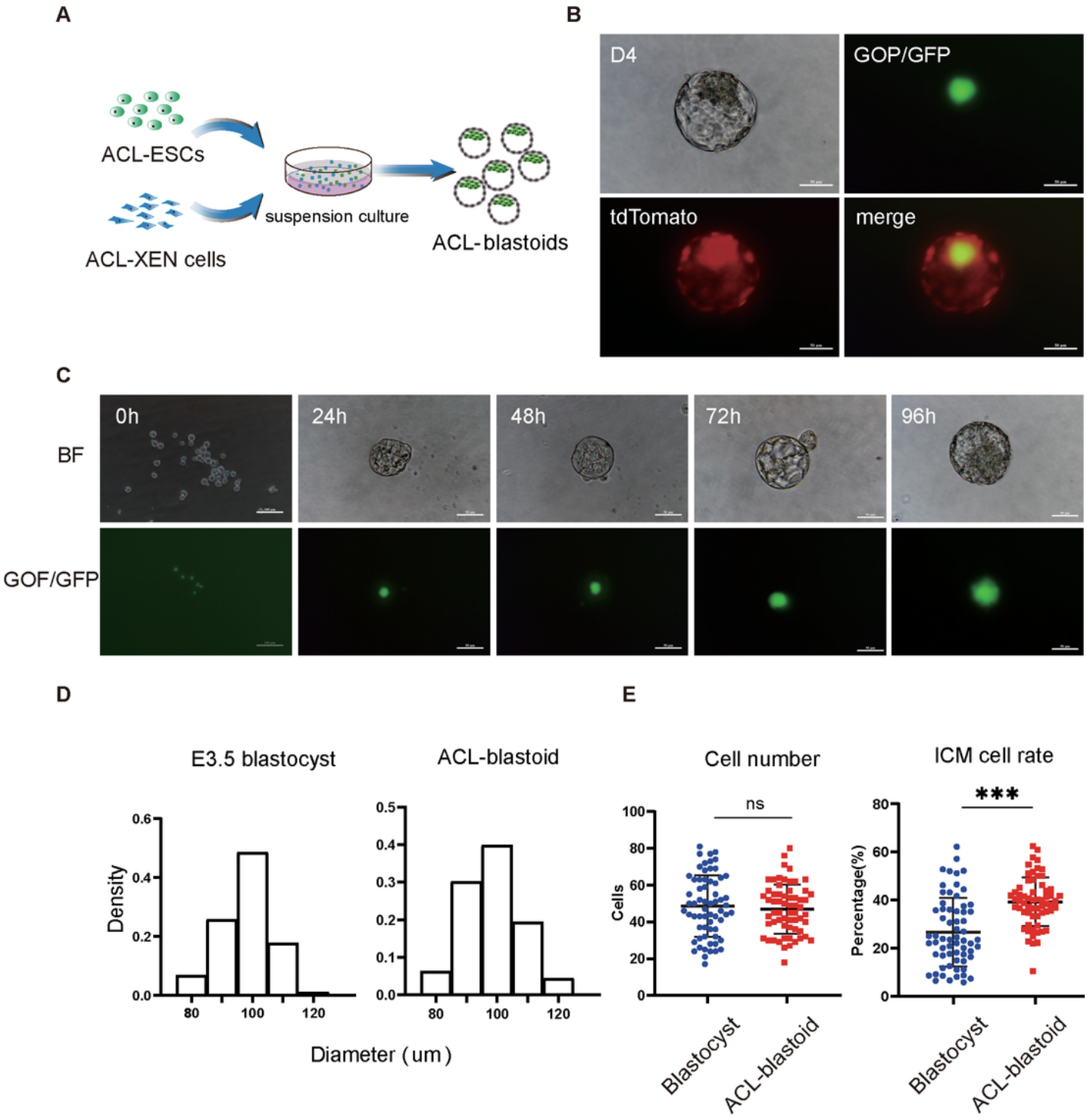

Figure 4

Generation of blastoid from ACL-ESCs and ACL-XEN cells.

A Diagram of self-assembly into ACL-blastoids with ACL-ESCs and ACL-XEN cells.

B Bright-field, fluorescent images and a merged live image of an ACL-blastoid at day 4 with ACL-ESCs (GOF/GFP+) and ACL-XEN cells (tdTomato+). Scale bar, 100 μm.

C Representative bright-field (top) and fluorescence images (bottom) of the formation process of ACL-blastoids at the indicated time point. Scale bar, 100 μm (0 h), 50 μm (24-96 h). BF, bright field.

D Histograms showing the distribution of diameter of 175 E3.5 blastocysts (top) and 206 ACL-blastoids (bottom).

E Total cell number and ICM cell ratio were quantified between 64 E3.5 blastocysts and 62 ACL-blastoids. Data are means ± SD, *p*** < 0.0001*.

Fig. 5

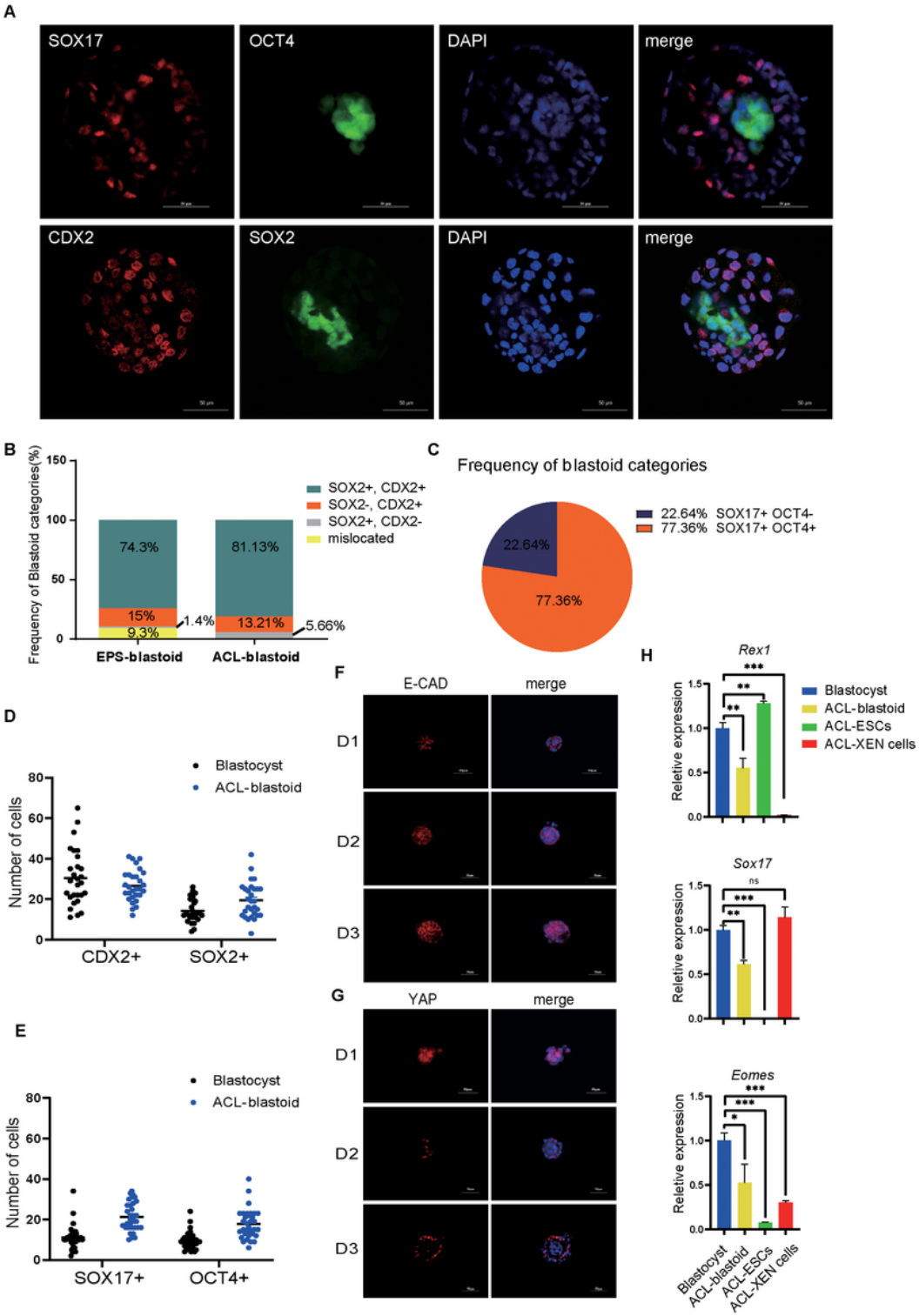

Figure 5

Lineage potency of ACL-blastoids.

A IF staining of OCT4, SOX2, SOX17 and CDX2 in ACL-blastoids cultured for 5 days. Below all ACL-blastoids be collected at day 5. DAPI stained the nucleus. Scale bars, 50 μm.

B The frequency of ACL-blastoid categories based on the expression of CDX2 and SOX2 in the chart. n = 53 ACL-blastoids, compared with previous published EPS-blastoid.

C The frequency of 53 ACL-blastoid categories based on the expression of SOX17 and OCT4 in the chart.

D Quantification of the cells number with SOX2+ or CDX2+ in 29 blastocysts and 28 ACL-blastoids.

E Quantification of the cells number with OCT4+ or SOX17+ in 36 blastocysts and 33 ACL-blastoids. DAPI stained the nucleus. Scale bars, 50 μm.

F Quantification of the cells number with OCT4+ or SOX17+ in 36 blastocysts and 33 ACL-blastoids. DAPI stained the nucleus. Scale bars, 50 μm.

G IF staining of Active-YAP (YAP) in early stage of ACL aggregates at the indicated time point. DAPI stained the nucleus. Scale bars, 50 μm.

H Relative expression of three blastocyst lineages genes (*Rex1*, *Sox17* and *Eomes*) measured by qPCR in individual blastocyst at day 4, ACL-blastoid at day 5, ACL-ESCs, ACL-XEN cells. Blastocyst was used as control. Error bars indicate means ± SD (n = 3). *p* values were calculated by unpaired two-tailed Student's *t* test, $p < 0.05$.

Fig. 6

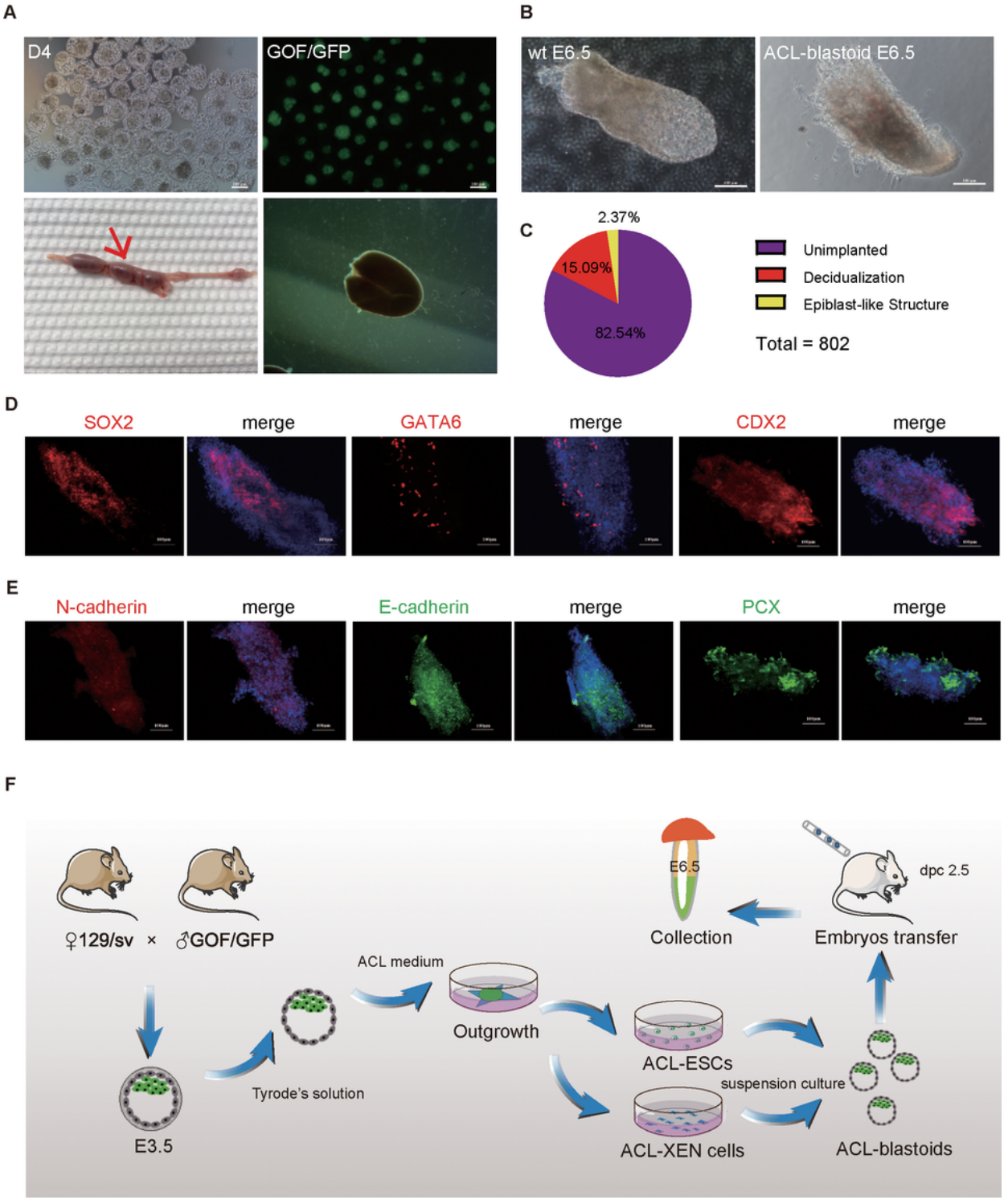

Figure 6

In vivo developmental potential of ACL-blastoids.

A The formation of E6.5 decidua in the mouse uterus after ACL-blastoids with GOF/GFP (top) transferred to 2.5 dpc recipient. Red arrow indicates deciduae. Scale bars, 50 μm.

B Left: wild type E6.5 gastrula. Right: *in vivo* ACL-blastoid developed to gastrulation-like structure and collected from deciduae at 6.5 dpc embryos. Scale bars, 50 μm.

C A pie chart showing the frequency of implantation capacity of ACL-blastoids. n = 802.

D IF staining of SOX2, GATA6 and CDX2 in tissue sections of *in vivo* ACL-blastoid developed to gastrulation-like structures and collected from deciduae at 7.5 dpc embryos. DAPI stained the nucleus. Scale bars, 50 μm.

E IF staining of N-cadherin, E-cadherin and PCX in tissue sections of *in vivo* ACL-blastoid developed to gastrulation-like structures and collected from deciduae at 7.5 dpc embryos. PCX, podocalyxin. DAPI stained the nucleus. Scale bars, 50 μm.

F Overview of generate ACL-blastoids with ACL-ESCs and ACL-XEN cells derived from one blastocyst, and followed by *in vivo* developmental potential of ACL-blastoid.

Supplementary Files

This is a list of supplementary files associated with this preprint. Click to download.

- SupplementaryFig.1.tif
- SupplementaryFig.2.tif
- SupplementaryFig.3.tif
- SupplementaryFig.4.tif
- SupplementaryFigurelegends.docx
- SupplementaryTable1.xlsx